Available online at www.sciencedirect.com
ScienceDirect
Journal of Solid State Chemistry 180 (2007) 484–488
JOURNAL OF SOLID STATE CHEMISTRY
www.elsevier.com/locate/jssc

The effect of B_2O_3 addition on the crystallization of amorphous TiO_2–ZrO_2 mixed oxide

Dongsen Mao*, Guanzhong Lu

Research Institute of Applied Catalysis, Department of Chemical Engineering, Shanghai Institute of Technology, Number 120, Caobaolu, Shanghai 200235, PR China

Received 13 July 2006; received in revised form 19 October 2006; accepted 6 November 2006
Available online 14 November 2006

Abstract

The effect of B_2O_3 addition on the crystallization of amorphous TiO_2–ZrO_2 mixed oxide was investigated by X-ray diffraction (XRD), thermogravimetric and differential thermal analysis (TG/DTA). TiO_2–ZrO_2 mixed oxide was prepared by co-precipitation method with aqueous ammonia as the precipitation reagent. Boric acid was used as a source of boria, and boria contents varied from 2 to 20 wt%. The results indicate that the addition of small amount of boria (<8 wt%) hinders the crystallization of amorphous TiO_2–ZrO_2 into a crystalline $ZrTiO_4$ compound, while a larger amount of boria ($\geqslant 8$ wt%) promotes the crystallization process. FT-IR spectroscopy and ^{11}B MAS NMR results show that tetrahedral borate species predominate at low boria loading, and trigonal borate species increase with increasing boria loading. Thus it is concluded that highly dispersed tetrahedral BO_4 units delay, while a build-up of trigonal BO_3 promote, the crystallization of amorphous TiO_2–ZrO_2 to form $ZrTiO_4$ crystals.

Keywords: Boria; TiO_2–ZrO_2 mixed oxide; Crystallization; Zirconium titanate

1. Introduction

Supported boria catalysts are widely used for various reactions such as vapor phase Beckmann rearrangement of cyclohexanone oxime [1], toluene disproportionation [2], isomerization of 1-butene [3], dehydration of alcohol [4], photocatalytic decomposition of water [5], and partial oxidation of methane using oxygen as the oxidant [6]. These catalysts are usually prepared by impregnating the boria from an aqueous solution of boric acid on an inorganic oxide support, such as SiO_2, Al_2O_3, TiO_2 and ZrO_2. It is well established in the literature that the type of support plays a key role in the catalytic performance and for a given reaction the activity, selectivity and stability of the catalyst can be improved greatly by the use of an appropriate support oxide [7].

In comparison with the single component supports, the composite oxide supports are usually found to exhibit higher surface acidity, surface area, and thermal and mechanical strength [8]. Among various mixed oxides, the titania–zirconia binary oxide has been reported to exhibit a high surface acidity by a charge imbalance based on the generation of Ti–O–Zr bonding [9]. It is also possible that Ti and Zr ions on the TiO_2–ZrO_2 may act as acidic and basic sites, respectively, which may serve as catalytic active sites [10]. Thus, the combined TiO_2–ZrO_2 mixed oxide has attracted much attention recently as a catalyst and support for various applications. Very recently, we have reported that a better catalytic performance of vapor phase Beckmann rearrangement of cyclohexanone oxime to ε-caprolactam, a commercially important product in the manufacture of synthetic fibers (especially nylon-6) and in many other applications, can be achieved on a TiO_2–ZrO_2 supported boria catalyst [11–13]. It gives rise to a higher ε-caprolactam yield and has a longer lifetime as compared with that of B_2O_3/TiO_2 and B_2O_3/ZrO_2 catalyst. Furthermore, we studied the effect of boria content on the catalytic performance of the B_2O_3/TiO_2–ZrO_2 catalysts in the range of 8–20 wt% and found that the highest conversion of oxime and selectivity of ε-caprolactam was obtained at the

*Corresponding author. Fax: +86 21 64945006.
E-mail addresses: dsmao1106@yahoo.com.cn, dsmao@sit.edu.cn (D. Mao).

0022-4596/$ - see front matter © 2006 Published by Elsevier Inc.
doi:10.1016/j.jssc.2006.11.009

boria content of 12 wt% [11]. These results are well interpreted in terms of the acidic and textural characteristics of the catalysts. In the present work, the effect of boria addition in a wider range (2–20 wt%) on the crystallization of TiO_2–ZrO_2 binary oxide support was studied by XRD and TG/DTA techniques, and related to the structure of dispersed boria characterized by XRD, FT-IR and ^{11}B MAS NMR techniques.

2. Experimental

2.1. Preparation

The TiO_2–ZrO_2 mixed oxide (1:1 molar ratio) support was prepared by a co-precipitation method using aqueous ammonia as the precipitation reagent as described previously [11]. In brief, an aqueous mixture solution containing the requisite quantities of titanium tetrachloride (AR grade, Shanghai Chemical Reagent Corporation, PR China) and zirconium oxychloride (AR grade, Shanghai Chemical Reagent Corporation, PR China) was added to an excess amount of aqueous ammonia slowly and mixed thoroughly by control of the final pH = 9. The precipitate thus obtained was allowed to stand at ambient temperature overnight, filtered, washed thoroughly with de-ionized water until no chloride ions were detected by adding $AgNO_3$ solution to the filtrate, and then dried at 110 °C overnight. The dried precipitate was finally calcined at 500 °C for 6 h.

The B_2O_3/TiO_2–ZrO_2 catalysts, with various boria loadings ranging from 2 to 20 wt% were prepared by pore-volume impregnation of TiO_2–ZrO_2 with aqueous solutions containing various amounts of boric acid (AR grade, Shanghai Chemical Reagent Corporation, PR China). Samples containing higher boria loadings (⩾8 wt%) were prepared by multi-step impregnation. Samples were dried at 110 °C for 4 h between impregnation steps. All samples in the series were finally dried at 110 °C overnight and then calcined at 600 °C for 12 h. The heating rate was always maintained at 10 °C/min.

2.2. Characterization

X-ray powder diffraction patterns of the samples were obtained with a Rigaku D/MAX-1400 diffractometer, which utilized nickel-filtered Cu$K\alpha$ radiation. Diffraction patterns were obtained with an X-ray gun operated at 40 kV and 40 mA, in the range of $2\theta = 5$–40° using a scanning rate of 15 °/min.

Thermogravimetric (TG) and differential thermal analysis (DTA) were carried out using a high temperature thermal analyzer (Dupont, TA-4000) in the presence of flowing air (50 ml/min) at a heating rate of 20 °C/min. Finely powdered alumina was used as a reference material. The samples used were the dried boric acid impregnated supports (110 °C, overnight) prior to calcination.

The FT-IR spectra were collected on a Bruker IFS-88 FT-IR spectrometer at room temperature and atmospheric pressure, using KBr discs, with a spectral resolution of 4 cm^{-1}.

^{11}B MAS NMR spectra were recorded at resonance frequency of 96.29 MHz on a Bruker DMX-300 multinuclear spectrometer, while a MAS spinner was rotated at a rate of 12 kHz, 8° rf pulses, 1 s recycle delay. Background subtraction was necessary due to boron nitride components in the probe. Chemical shifts reported in parts per million (ppm) were referenced to BF_3 etherate.

3. Results and discussion

3.1. XRD measurements

In a previous paper [11] we have studied the crystal structures of TiO_2–ZrO_2 (1:1) samples calcined at different temperatures from 500 to 1000 °C. The results indicate that after calcining at 500 °C, the TiO_2–ZrO_2 mixed oxide is in an amorphous state. However, X-ray diffraction lines characteristic of the formation of the crystalline $ZrTiO_4$ compound can be observed from 600 °C and above temperatures, and whose crystallinities increase with an increase in calcination temperature. This result was consistent with those reported earlier by Daly et al. [14] and Reddy et al. [15]. On the other hand, Noguchi and Mizuno [16] reported that tetragonal and monoclinic ZrO_2, and rutile TiO_2 could be produced by the decomposition of $ZrTiO_4$ at higher temperatures. Wu et al. [9] also found that relatively important amounts of TiO_2 (rutile) phase were separated from $ZrTiO_4$ at higher calcination temperatures (⩾850 °C). Furthermore, Navio and co-workers [17] detected the formation of TiO_2 in rutile phase even after calcination at 500 °C. As suggested by Reddy et al. [15], the observed higher stability of $ZrTiO_4$ compound may presumably be due to a different preparation method adopted and the precursor compounds used for the preparation of this mixed oxide in the present study.

The representative XRD patterns of B_2O_3/TiO_2–ZrO_2 catalysts with various boria loadings are depicted in Fig. 1. As can be seen from this figure, the B_2O_3/TiO_2–ZrO_2 catalysts with lower boria loadings (<8 wt%) are in X-ray amorphous states. However, crystalline $ZrTiO_4$ is already formed for TiO_2–ZrO_2 without addition of B_2O_3 after calcination at the same temperature (600 °C) [11]. From these results, it is concluded that the incorporation of small amount of boron hinders effectively the crystallization of the amorphous TiO_2–ZrO_2. On the other hand, when the boria loading increases to ⩾8 wt%, the diffraction lines due to the formation of $ZrTiO_4$ compound are observed again. Moreover, the intensities of these bands increase with boria loading. This result indicates that the transformation of amorphous TiO_2–ZrO_2 mixed oxide into a crystalline $ZrTiO_4$ compound is accelerated by the supported boria. The results described above suggest that the addition of boria with different content has different effect

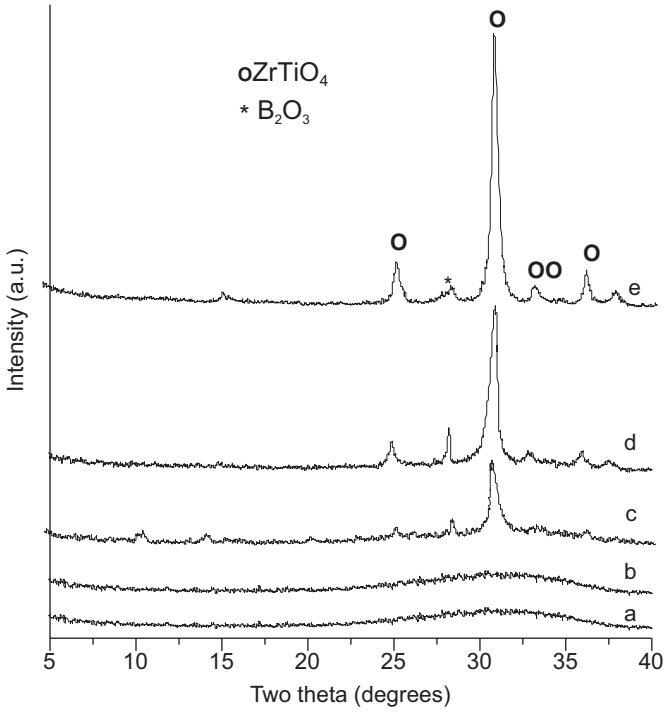

Fig. 1. XRD patterns of B_2O_3/TiO_2–ZrO_2 catalysts with various boria loadings calcined at 600 °C: (a)2 wt%, (b) 5 wt%, (c) 8 wt%, (d) 10 wt%, (e) 20 wt%.

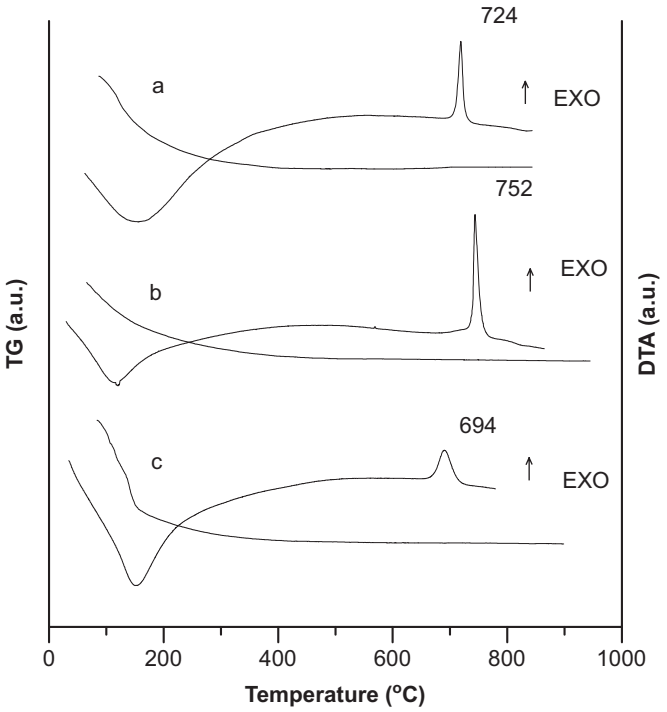

Fig. 2. TG and DTA profiles of TiO_2–ZrO_2 support (a) and B_2O_3/TiO_2–ZrO_2 catalysts with 5 wt% boria (b) and 20 wt% (c) dried at 110 °C.

on the crystallization of amorphous TiO_2–ZrO_2: the small amount of boria hinders the crystallization process, whilst the higher loading promotes the transformation. This is an interesting observation from the present study. To our best knowledge, this peculiar effect of boria on the crystallization of amorphous oxide has never been reported so far.

In addition, as shown in Fig. 1, the characteristic peak of crystalline B_2O_3 ($2\theta = 28^\circ$) is only observed in the X-ray diffraction patterns of the B_2O_3/TiO_2–ZrO_2 catalysts with higher boria loadings ($\geqslant 8$ wt%). This result suggests that B_2O_3 below 8 wt% loading is in a highly dispersed and amorphous state. Moreover, the intensity of the diffraction line of crystalline B_2O_3 is almost the same for the catalysts containing more than 8 wt% B_2O_3, i.e., regardless of the boria loading. The above result shows the formation of surface amorphous B_2O_3 phases as predominant species on the B_2O_3/TiO_2–ZrO_2 catalysts in the range of B_2O_3 content examined here (2–20 wt%). In this sense, boria is known to be one of the most difficult substances to crystallize [18].

3.2. Thermal analysis (TG/DTA)

The TG and DTA profiles of B_2O_3/TiO_2–ZrO_2 catalysts with boria loadings of 5 and 20 wt% are shown in Fig. 2, where those of the TiO_2–ZrO_2 support obtained under the same conditions are also depicted for comparison. The TG profiles are characterized by a weight loss up to 400 °C. Below 400 °C the weight loss, accompanied by a endothermic peak with maximum at 110–160 °C in the DTA profile, can be attributed to the desorption of physically adsorbed water and the dehydration of H_3BO_3. Because the water physically adsorbed on catalysts is more easily removed than that produced by dehydration of boric acid, the maximum of the peak shifts towards higher temperatures with increasing the B_2O_3 loading, i.e., from about 120 °C for 5 wt% B_2O_3 to about 150 °C for 20 wt% B_2O_3. At the same time, the intensity of the endothermic peak increases with an increase in the B_2O_3 loading. Izumi et al. [2] also reported that the alumina–boric acid systems with boria loading $\leqslant 20$ wt% give one broad endothermic peak at about 130 °C. They proposed that boric acid is dehydrated to form metaboric acid as an intermediate and that it reacts with an active anhydrous alumina at about 130 °C, while excessive boric acid is transferred into isolated boria which exhibits a peak at around 180 °C in the DTA profile. Moreover, all of the DTA profiles show an exothermic band without a corresponding TG peak. From this observation, it is concluded that the exothermic transition corresponds to a crystallization of the amorphous TiO_2–ZrO_2. The phase transition from amorphous to $ZrTiO_4$ crystalline phase is detected at around 724 °C for TiO_2–ZrO_2 support. This result is in good accordance with that (712 °C) reported recently by Zou et al. [19]. But the XRD characterization results presented above reveal well-crystalline material, even significantly below this temperature. This may be due to the role of the calcination period, which plays an important role in phase transition [20]. It has to be taken into account that this is dynamic value on heating, while sample calcined in static air was used for XRD analysis. Therefore, a comparison of DTA results with

those of XRD may be misleading. A similar observation was also recently made by Sham et al. [21].

In addition, it is clear that the addition of boria exerts significant effect on the position of this exothermic peak. For B_2O_3/TiO_2–ZrO_2 catalyst with boria loading of 5 wt%, the exothermic peak increases to 752 °C from 724 °C of TiO_2–ZrO_2 support. However, for the samples with higher boria loadings (⩾8 wt%), the exothermic peak shifts to lower temperatures and thus, for a 20 wt% B_2O_3, it appears at 694 °C (30 °C lower than that of TiO_2–ZrO_2 support). These results support our conclusion deduced from the above XRD measurements, viz. the small amount of boria retards the crystallization of amorphous TiO_2–ZrO_2, whilst the higher loading promotes the transformation process.

3.3. Characterization of B_2O_3 structure

The different effect of boria with different loadings on the crystallization process of the amorphous TiO_2–ZrO_2 may be related to the different interaction between boria and TiO_2–ZrO_2 which can be reflected by the different states of boron on the surface of catalysts. It is well known that there exist two structure units (i.e. tetrahedral BO_4 and trigonal BO_3) of boron in borates [1–4,7,18,22,23]. FT-IR [2,4,7,18] and ^{11}B MAS NMR [1,3,18,22,23] technologies have been extensively used to ascertain the nature of the B_2O_3 structure existing on various supports.

3.3.1. FT-IR study

The representative FT-IR spectra of the B_2O_3/TiO_2–ZrO_2 catalysts with various B_2O_3 loadings in the skeletal region (2500–400 cm^{-1}) are shown in Fig. 3. As shown in Fig. 3, the sample with 5 wt% B_2O_3 shows three weak broad bands at 1400–1430, 1300–1400 and 1050–1150 cm^{-1}, respectively. As the boria loading increases, the band at 1400–1430 cm^{-1} shifts up to 1460 cm^{-1}, and the intensity of this band increases gradually. At the same time, the bands at 1300–1400 and 1050–1150 cm^{-1} disappear. Furthermore, two new bands are observed at about 1190 and 880 cm^{-1}, respectively, whose intensities increase with the increase in boria loading. The band near 1650 cm^{-1} is due to the scissoring-mode of water molecules, probably involved in H-bonding, as proposed by Delmastro et al. [4].

Information on the structure of the borate species present on B_2O_3/TiO_2–ZrO_2 catalysts can be obtained from the above spectra, taking into account the characteristic spectra of the different boron–oxygen compounds. By comparison with the spectra of boric acid (only BO_3 units) and borax (both BO_3 and BO_4 units), it is concluded that the bands at 1460, 1190 and 880 cm^{-1} represent the formation of BO_3 units, while the bands at 1300–1400 and 1050–1150 cm^{-1} represent the formation of BO_4 units [24]. The spectra of B_2O_3/TiO_2–ZrO_2 samples show that in these materials both tetrahedral and trigonal boron species exist on their surface. Moreover, the coordination of boron atoms in the samples with lower B_2O_3 loadings is mainly in BO_4 units. However, in the samples with higher boria loadings, the boria is constructed predominantly by BO_3 units, and the amount of these BO_3 units increases with increasing the boria loading.

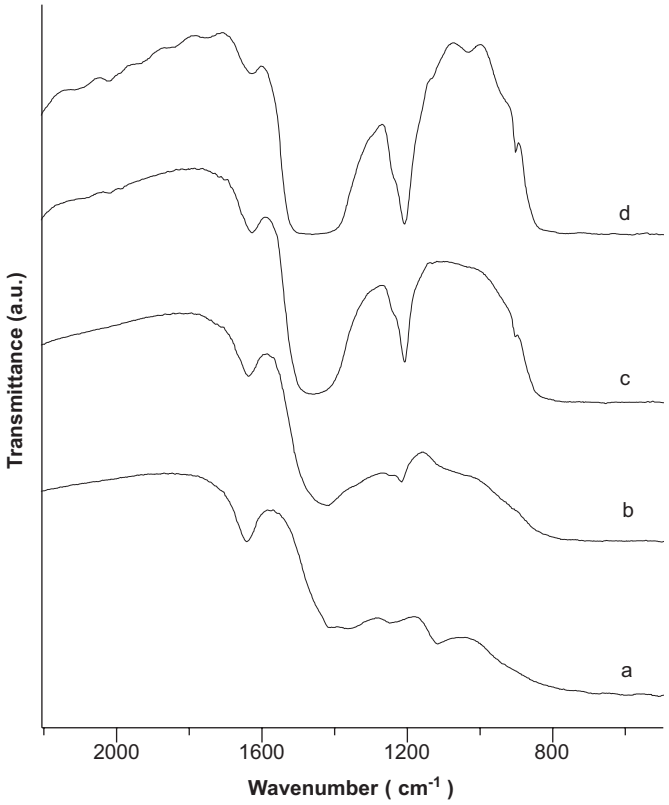

Fig. 3. IR spectra of B_2O_3/TiO_2–ZrO_2 catalysts with various B_2O_3 loadings: (a) 5 wt%, (b) 8 wt%, (c) 12 wt%, (d) 20 wt%.

3.3.2. ^{11}B MAS NMR study

It is well known that tetrahedral BO_4 and trigonal BO_3 units have similar isotropic chemical shifts but substantially different quadrupolar coupling constants. Under MAS at high magnetic fields, the ^{11}B NMR spectra of tetrahedral BO_4 units usually give a relatively narrow single signal in the range −5 to 2 ppm from boron trifluoride etherate ($BF_3 \cdot EtO_2$), indicating a highly symmetrical arrangement of the four oxygen atoms in the BO_4 tetrahedron in the framework. Furthermore, trigonal BO_3 units produce a characteristic quadrupolar doublet pattern due to its high quadrupolar interaction. Because the ^{11}B chemical shift range is small, the peaks corresponding to the two boron coordinations often cannot be clearly separated. Hence, rapid sample spinning (⩾6 kHz) together with high power proton decoupling is desirable for acquisition of ^{11}B NMR spectra of borates and borosilicates, from which accurate trigonal/tetrahedral ratios may be determined [18].

Fig. 4 presents some of the ^{11}B MAS NMR spectra of B_2O_3/TiO_2–ZrO_2 catalysts with different boria loadings. As shown, all the samples consist of both trigonal and tetrahedral B–O coordinations. With an increase in boria

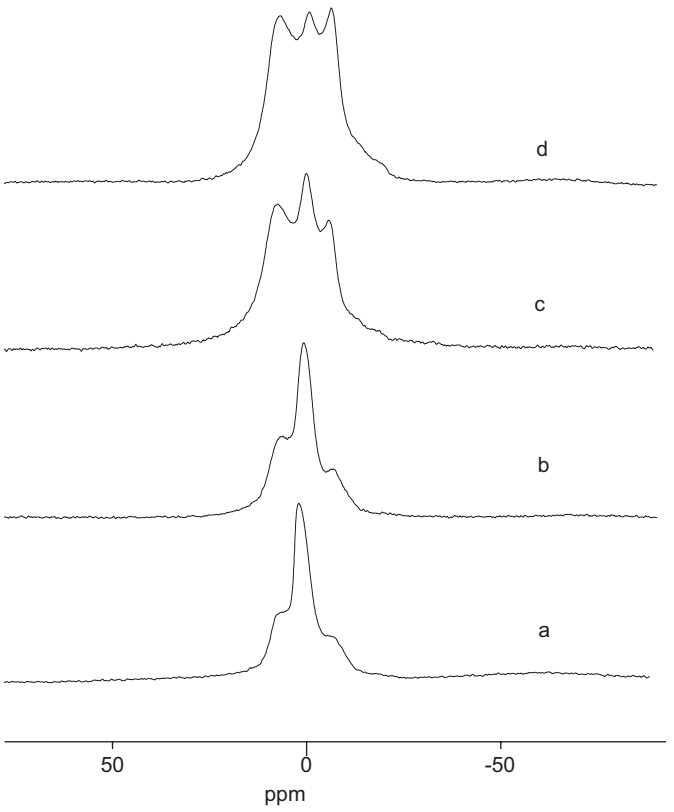

Fig. 4. ^{11}B MAS NMR spectra of B_2O_3/TiO_2–ZrO_2 catalysts with various boria loadings: (a) 5 wt%, (b) 8 wt%, (c) 12 wt%, (d) 20 wt%.

loading, the intensity of tetrahedral signal decreases but that of trigonal signal increases. Thus, the ratio of BO_3 to BO_4 species increases with increasing boria loading, which is well in agreement with that found in FT-IR study. Based on the above results, we conclude that the difference in the structure of boria on the surface of B_2O_3/TiO_2–ZrO_2 catalysts with different boria loadings reveals the different interactions between boria and TiO_2–ZrO_2, which may lead to the different effect on the crystallization process of the amorphous TiO_2–ZrO_2. Furthermore, connecting the crystalline structure of the B_2O_3/TiO_2–ZrO_2 catalysts with different boria loadings with their behavior in the vapor phase Beckmann rearrangement of cyclohexanone oxime [25] we suggest that the presence of crystalline $ZrTiO_4$ is favorable for the selective synthesis of ε-caprolactam.

4. Conclusions

The TiO_2–ZrO_2 binary oxide support, when calcined at 500 °C, is in an X-ray amorphous state. The amorphous TiO_2–ZrO_2 transforms into crystalline $ZrTiO_4$ compound beyond 600 °C calcination temperatures and this compound is thermally quite stable even up to 1000 °C. The crystallization process of the initially amorphous TiO_2–ZrO_2 is hindered by the incorporation of low content of boron, whilst favored by high content of boron.

Acknowledgement

We gratefully acknowledge Shanghai Research Institute of Petrochemical Technology (SRIPT), SINOPEC, for the financial support. The authors would like to express their sincere gratitude to those who contributed to this research: Mr. Zhu Ming for XRD measurements, Mrs. Zhu Zhiqiang for TG/DTA analysis and Mr. Lu Liyuan for FT-IR tests.

References

[1] L. Forni, G. Fornasari, C. Tosi, F. Trifirò, A. Vaccari, F. Dumeignil, J. Grimblot, Appl. Catal. A 248 (2003) 47–57.
[2] Y. Izumi, T. Shiba, Bull. Chem. Soc. Jpn. 37 (1964) 1797–1809.
[3] S. Sato, M. Kuroki, T. Sodesawa, F. Nozaki, G.E. Maciel, J. Mol. Catal. A 104 (1995) 171–177.
[4] A. Delmastro, G. Gozzelino, D. Mazza, M. Vallino, G. Busca, V. Lorenzelli, J. Chem. Soc., Faraday Trans. 88 (1992) 2065–2070.
[5] S.C. Moon, H. Mametsuka, S. Tabata, E. Suzuki, Catal. Today 58 (2000) 125–132.
[6] K. Otsuka, M. Hatano, J. Catal. 108 (1987) 252–255.
[7] B.Q. Xu, S.B. Cheng, S. Jiang, Q.M. Zhu, Appl. Catal. A 188 (1999) 361–368.
[8] J.B. Miller, S. Rankin, E.I. Ko, J. Catal. 148 (1994) 673–682.
[9] J.C. Wu, C.S. Chung, C.L. Ay, I. Wang, J. Catal. 87 (1984) 98–107.
[10] J. Fung, I. Wang, J. Catal. 164 (1996) 166–172.
[11] D.S. Mao, G.Z. Lu, Q.L. Chen, Z.K. Xie, Y.X. Zhang, Catal. Lett. 77 (2001) 119–124.
[12] D.S. Mao, G.Z. Lu, Q.L. Chen, React. Kinet. Catal. Lett. 75 (2002) 75–80.
[13] D.S. Mao, Q.L. Chen, G.Z. Lu, Appl. Catal. A 244 (2003) 273–282.
[14] F.P. Daly, H. Ando, J.L. Schmitt, E.A. Sturm, J. Catal. 108 (1987) 401–408.
[15] B.M. Reddy, B. Manohar, S. Mehdi, J. Solid State Chem. 97 (1992) 233–238.
[16] T. Noguchi, M. Mizuno, Sol. Energy 11 (1967) 56.
[17] J.A. Navio, F.J. Marchena, M. Macias, P.J. Sanchez-Soto, P. Pichat, J. Mater. Sci. 27 (1992) 2463.
[18] F.M. Bautista, J.M. Campelo, A. Garcia, D. Luna, J.M. Marinas, M.C. Moreno, A.A. Romero, J.A. Navio, M. Macias, J. Catal. 173 (1998) 333–344.
[19] H. Zou, Y.S. Lin, Appl. Catal. A 265 (2004) 35–42.
[20] D. Das, H.K. Mishra, K.M. Parida, A.K. Dalai, J. Mol. Catal. A 189 (2002) 271–282.
[21] E.L. Sham, M.A.G. Aranda, E.M. Farfan-Torres, J.C. Gottifredi, M. Martinez-Lara, S. Bruque, J. Solid State Chem. 139 (1998) 225–232.
[22] K.P. Peil, L.G. Galya, G. Marcelin, J. Catal. 115 (1989) 441–451.
[23] C. Flego, W.O. Parker Jr., Appl. Catal. A 185 (1999) 137–152.
[24] D.S. Mao, G.Z. Lu, Q.L. Chen, J. Mol. Catal. A 240 (2005) 164–171.
[25] D.S. Mao, G.Z. Lu, Q.L. Chen, Z.K. Xie, Y.X. Zhang, Chinese J. Catal. 23 (2002) 9–14.